Nanoscale Research Letters
a SpringerOpen Journal

NANO EXPRESS Open Access

In situ-grown hexagonal silicon nanocrystals in silicon carbide-based films

Tae-Youb Kim[1*], Chul Huh[1], Nae-Man Park[1], Cheol-Jong Choi[2] and Maki Suemitsu[3*]

Abstract

Silicon nanocrystals (Si-NCs) were grown *in situ* in carbide-based film using a plasma-enhanced chemical vapor deposition method. High-resolution transmission electron microscopy indicates that these nanocrystallites were embedded in an amorphous silicon carbide-based matrix. Electron diffraction pattern analyses revealed that the crystallites have a hexagonal-wurtzite silicon phase structure. The peak position of the photoluminescence can be controlled within a wavelength of 500 to 650 nm by adjusting the flow rate of the silane gas. We suggest that this phenomenon is attributed to the quantum confinement effect of hexagonal Si-NCs in silicon carbide-based film with a change in the sizes and emission states of the NCs.

Keywords: Silicon nanocrystals, *in situ*-formed Si-NCs, Silicon carbide-based films, Hexagonal silicon phase structure

Background

Silicon-related low-dimensional structures such as Si nanocrystals (Si-NCs) have shown great potential in the development of next-generation devices. When Si-NCs are made smaller than the free-exciton Bohr radius of bulk Si, they behave as quantum dots [1-3] with various energy states that can be tuned using carrier confinement in all three dimensions. These quantum properties of Si-NCs have the greatest impact when they are embedded in a wide-gap dielectric matrix, the structure of which is quite intriguing in the field of Si optoelectronics and third-generation photovoltaics [4,5].

Among such wide-gap dielectric matrices for optoelectronic and photovoltaic devices are Si carbide-based films. These films are considered to have one of the most promising top (window) layers due to a high transparency to photons absorbed by an underneath layer of Si-based junctions as well as to the conductive nature of the material. Moreover, when Si carbide-based film includes Si-NCs, the combination will certainly have further advantages. One such advantage is a lower barrier height caused by a lower bandgap of Si carbide (approximately 2.5 eV) compared to Si oxide (approximately 9 eV) and Si nitride (approximately 5.3 eV), which brings about an increased tunneling probability between Si-NCs [5-7]. Other advantages include the easy formation of minibands between Si-NCs and a higher Bloch carrier mobility [3,8].

To fabricate Si-NCs in Si carbide-based dielectric matrix structures, high-temperature (T > 1,100°C) post-deposition annealing of a Si-containing amorphous dielectric film (i.e., Si oxide, Si nitride, and Si carbide) has been commonly used. However, this high-temperature process may pose a serious challenge in the development of a device fabrication process [9]. In this regard, we have developed a method for the *in situ* fabrication of Si-NCs during the deposition of Si nitride-based matrices [10-12]. However, no attempt has yet been made to create a Si carbide-based matrix, which forms the motivation of this study.

Another interesting subject related to the formation of Si-NCs is the control of Si polytypes [13-15]. It is well known that Si crystallizes into a cubic-diamond structure under normal growth and treatment conditions. However, Si is also known to have several polytypes that are stable only at high pressure. Among these Si polytypes, hexagonal-wurtzite Si is important as it sometimes appears in stressed amorphous Si and has enhanced non-linear optical properties for novel optoelectronic applications [13-15].

* Correspondence: youby@etri.re.kr; suemitsu@riec.tohoku.ac.jp
[1]Convergence Components and Materials Laboratory, Electronics and Telecommunications Research Institute (ETRI), Daejeon 305-700, Republic of Korea
[3]Research Institute of Electrical Communication, Tohoku University, Sendai 980-8577, Japan
Full list of author information is available at the end of the article

Springer

© 2012 Kim et al.; licensee Springer. This is an Open Access article distributed under the terms of the Creative Commons Attribution License (http://creativecommons.org/licenses/by/2.0), which permits unrestricted use, distribution, and reproduction in any medium, provided the original work is properly cited.

In this study, we demonstrate the *in situ* formation of hexagonal Si-NCs during the preparation of a silicon carbide-based matrix film at 250°C. The optical gaps of the Si-NCs have been characterized using photoluminescence (PL). Finally, we discuss the size effect of hexagonal Si-NC on its quantum confinement of carriers.

Methods

Plasma-enhanced chemical vapor deposition (PECVD) [10,12] with methane (CH_4, >99.999%) and silane (Ar-diluted SiH_4, >99.9999%) as the reactant gases has been employed to form a Si carbide-based dielectric film. Oxygen atoms are incorporated from the ambient environment, as we will see later. The total pressure and power of the plasma are 0.5 Torr and 5 W, respectively. The use of this low plasma power and highly diluted source gas is proven to be essential in the *in situ* formation of Si-NCs in amorphous Si and Si nitride-based matrices [10,12]. A Si(100) wafer was employed as the sample substrate, whose temperature during deposition was fixed at 250°C. The CH_4 flow rate was fixed at 10 sccm, while the SiH_4 flow rate was varied from 10 to 60 sccm to modulate the growth rate of the film. This variation in the SiH_4 flow rate controls the size of the Si-NCs. The size and crystallinity of the Si-NCs were characterized through high-resolution transmission electron microscopy (HRTEM) using a Tecnai G2 F20 instrument (FEI Co., Hillsboro, OR, USA) operated at 200 kV. To investigate the energy band of the Si-NCs, we conducted PL measurements at room temperature using a He-Cd (325 nm) laser for the excitation. The chemical composition of the matrix film was investigated using Fourier-transformed infrared spectroscopy (FTIR; IFS66V/S and HYPERION 3000, Bruker, Ettlingen, Germany).

Results and discussion

Figure 1a,c shows HRTEM images of the deposited film. In Figure 1a, the sample was grown using the gas flow rates of SiH_4/CH_4 = 20:10 sccm, and the average size of the Si-NCs is approximately 7 nm. In Figure 1c, the sample was grown using the gas flow rates of SiH_4/CH_4 = 60:10 sccm, and the average size of the Si-NCs is approximately 9 nm. Most of the Si-NCs are in a crystalline state, as evidenced by the lattice fringe shown in the HRTEM image as well as from the spotty pattern shown in the selected area of electron diffraction from one of the crystallites (Figure 1b). The diffraction pattern was determined to be caused by a (0001)-oriented hexagonal Si crystal [14,16]. From the diffraction pattern, the plane separation is determined to be d(10 $\bar{1}$ 0) = 3.31 Å, which is in good agreement with the established value (3.29 Å) for the hexagonal Si phase (JCPDS: Powder Diffraction File #80-0005).

The chemical composition of the dielectric matrix changes with the SiH_4 flow rate. Figure 2 shows a series of FTIR spectra for three different SiH_4 flow rates. The intense absorption bands at 780 to 800 cm^{-1} and 1,030 to 1,040 cm^{-1} are assigned to the Si-C and Si-O stretching modes [17,18], while the bands at 1,250 to 1,260 cm^{-1} and 2,120 to 2,150 cm^{-1} are assigned to the $Si\text{-}CH_3$ and Si-H stretching modes [17-19]. The dominance of the Si-O band, as well as the absence of C=O bonds (approximately 1,700 cm^{-1}), indicates that the film is of a Si carbide-based matrix with most of the oxygen atoms bonded to Si atoms. Although we do not exclude the

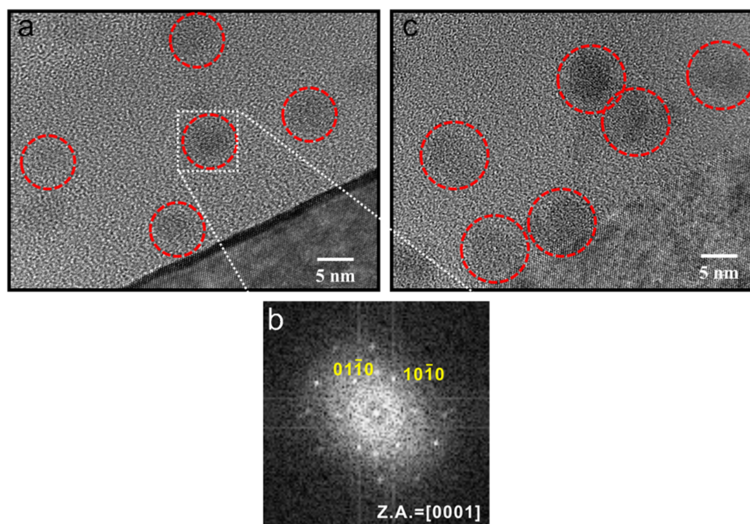

Figure 1 Cross-sectional HRTEM images of the Si-NCs embedded in a silicon carbide-based film. (**a**) Approximately 7-nm and (**c**) approximately 9-nm Si-NCs, enclosed by red circles for easy identification. (**b**) Selected area of the electron diffraction pattern from the portion indicated in (a). Presence of (0001)-oriented crystallites of the hexagonal silicon phase is confirmed.

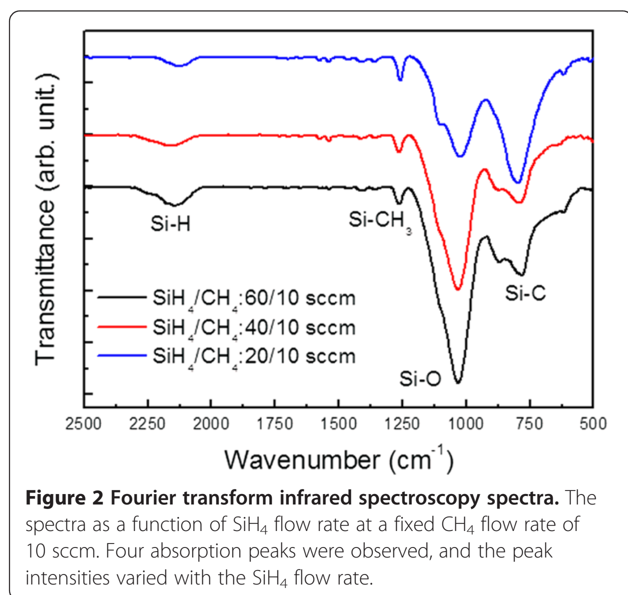

Figure 2 Fourier transform infrared spectroscopy spectra. The spectra as a function of SiH_4 flow rate at a fixed CH_4 flow rate of 10 sccm. Four absorption peaks were observed, and the peak intensities varied with the SiH_4 flow rate.

presence of Si-O-C bonding, its absorption peak at 1,125 cm^{-1} is very faint. The incorporation of oxygen atoms may be due either to the low purity of the nitrogen gas used to vent the reactor chamber or to the incorporation of oxygen atoms from the rather high (10^{-1} Pa) base pressure of the PECVD system. The very slow (<2 nm min^{-1}) growth condition necessary to realize the *in situ* formation of Si-NCs [10,20,21] accelerates the incorporation of oxygen atoms. However, the Si-O peak intensity increases with the SiH_4 flow rate. This is best understood in terms of the stronger bonding between Si and O atoms, which can be observed in these very slow growth conditions.

The growth mechanism of Si-NCs in a Si carbide-based film may be identical to the *in situ* formation of Si-NCs in amorphous Si [20] and Si nitride-based matrix films [10,12]. Namely, the key condition is the low rate of film growth, which can be acquired by low plasma power as well as by a high dilution of the source gas. Under optimum conditions, the Si nanoparticles are dispersedly formed in the matrix films during the film growth [12,20,21]. The Si nanoparticles formed are then transformed into nanocrystalline Si by hydrogen radical diffusion from the amorphous Si nanoparticles [10,12]. It is then likely that the structure of the Si-NCs is influenced by their surrounding matrix at the moment of crystallization. Namely, one possible mechanism for the formation of hexagonal-wurtzitic Si-NCs is the surrounding oxygen and carbon atoms (network) inducing sufficient stresses on the nuclei [13,15].

One of the most intriguing electronic properties in semiconducting nanostructures is the tunability of the bandgap based on their sizes. Figure 3a shows a series of PL spectra obtained for materials grown using SiH_4 flow rates of 10, 20, 40, and 60 sccm with a fixed CH_4 flow

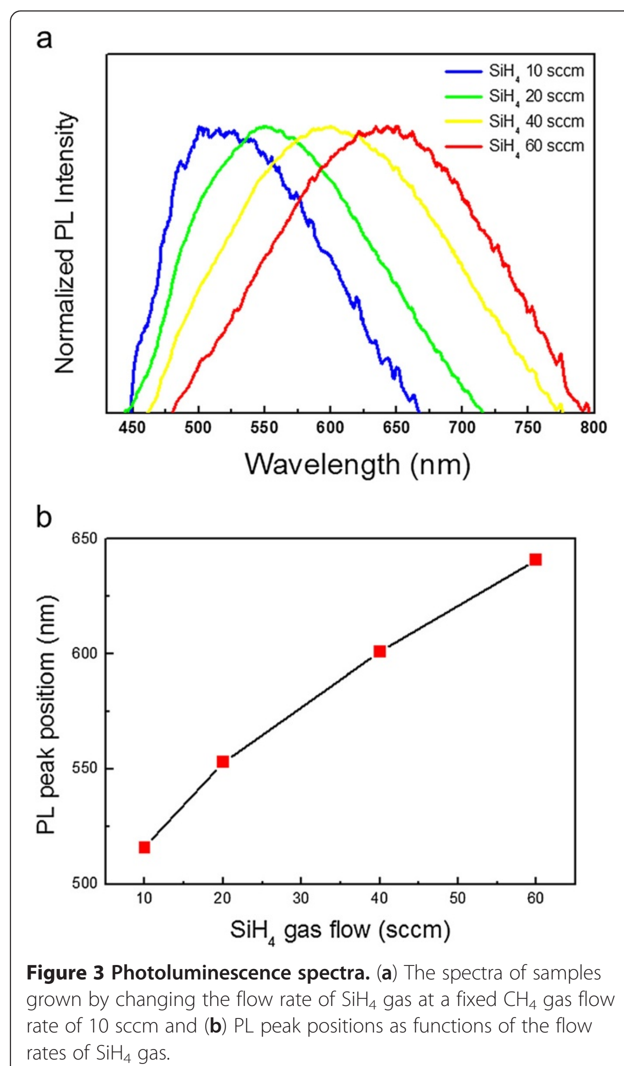

Figure 3 Photoluminescence spectra. (**a**) The spectra of samples grown by changing the flow rate of SiH_4 gas at a fixed CH_4 gas flow rate of 10 sccm and (**b**) PL peak positions as functions of the flow rates of SiH_4 gas.

rate of 10 sccm. With an increase in the silane flow rate, the peak position shows a redshift (see also Figure 3b). The possible origin of the PL emission is three-fold in our samples: (1) recombination at Si dangling bonds of defects, (2) recombination in the surrounding amorphous SiC-based matrix, and (3) recombination between quantized conduction and valence band states within the Si-NCs. Among the three, the first possible origin is denied because Si dangling bonds cannot have the observed variation in the PL energy [22]. The second possible origin is also denied because the optical bandgap of a-SiC-based film, and hence the PL energy, should increase with the incorporation of carbon or oxygen into the matrix in this model [23,24]. As we will see in Figure 4, however, the PL energy decreases with the increase of the oxygen content in the matrix.

We suggest the third possibility, the quantum confinement effect, being the most likely origin of the PL emission. As we have seen in Figure 1a,c, the PL redshift

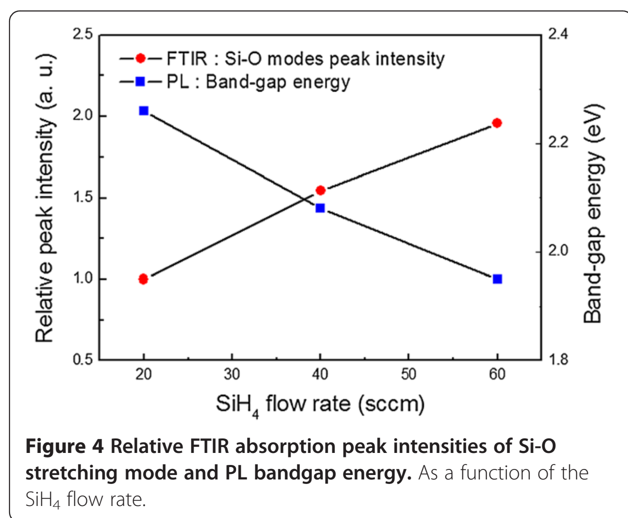

Figure 4 Relative FTIR absorption peak intensities of Si-O stretching mode and PL bandgap energy. As a function of the SiH_4 flow rate.

with increasing SiH_4 flow rate (Figure 3b) is accompanied by enlargement of the Si-NC size. This tendency between the PL energy versus Si-NC size d is consistent with the reported value based on the quantum confinement effect of $A + B/d$^2 with A = 1.475 eV and B = 38.5 (A is the bulk bandgap of the hexagonal crystal silicon, and B is the confinement parameter) [10,13,21], although further HRTEM observations are needed to determine the intermediate d values required for a more detailed analysis. Still, this A value is in reasonable agreement with the theoretical value of the direct-gap energy of approximately 1.48 eV by Joannopoulos and Cohen [25] and the experimental value (PL gap energy) of approximately 1.45 [13] both for hexagonal-wurtzite Si crystal.

The FTIR results of the Si-O peak intensity and PL spectra provide further support for the dominance of the quantum confinement effect. Figure 4 shows the relative FTIR absorption peak intensities of the Si-O stretching mode and the PL bandgap energy as a function of the SiH_4 flow rate. As the SiH_4 flow increases, the PL energy decreases while the Si-O mode intensity increases. Increasing the Si-O peak intensity means the increase of the oxygen content in the matrix, and it means the increase of the optical bandgap. The lowering of the PL energy, however, despite the increase of the oxygen content in the matrix, clearly indicates the dominance of the quantum confinement effect in determining the PL energy of the Si-NCs. We can therefore suggest that the hexagonal Si-NCs may have a tunable bandgap energy based on their size through the quantum confinement effect.

Conclusions

We investigated the *in situ* formation of Si-NCs during the growth of the surrounding Si carbide-based film through PECVD using methane (CH_4) and silane (SiH_4). No post-annealing process is necessary. The HRTEM measurements and PL results indicate the formation of Si-NCs with a hexagonal structure and good tunability of the optical bandgap under the growth conditions. The blueshift in the PL peak with a decreasing SiH_4 flow rate can be attributed to the three-dimensional quantum confinement effect in the hexagonal Si-NCs. These results demonstrate the viable potential of this method for the fabrication of silicon-based third-generation photovoltaics.

Competing interests

The authors declare that they have no competing interests.

Authors' contributions

TYK and MS designed the study and carried out the experiments. TYK, CH, NMP, and CJC performed the treatment of experimental data and calculations. TYK, CH, NMP, and MS took part in the discussions of the results and prepared the manuscript initially. All authors read and approved the final manuscript.

Acknowledgments

The authors sincerely thank Dr. Hu Young Jeong (Graduate School of EEWS at KAIST) for conducting the electron diffraction analysis. This research was supported by the Research & Development Improvement Program for ETRI (project number 10041416) funded by MKE/KEIT and the R&D program of ETRI (11BF1300, Project Planning of Convergence System Components and Material Technology) in Korea.

Author details

[1]Convergence Components and Materials Laboratory, Electronics and Telecommunications Research Institute (ETRI), Daejeon 305-700, Republic of Korea. [2]Department of Semiconductor Science and Technology, Chonbuk National University, Jeonju 561-756, Republic of Korea. [3]Research Institute of Electrical Communication, Tohoku University, Sendai 980-8577, Japan.

Received: 14 July 2012 Accepted: 9 October 2012
Published: 21 November 2012

References

1. Pavesi L, Lockwood DJ: *Silicon Photonics: Silicon Fundamentals for Photonic Applications*. Heidelberg: Berlin; 2004.
2. Walters RJ, Bourianoff GI, Atwater HA: **Field-effect electroluminescence in silicon nanocrystals.** *Nature Material* 2005, **4:**143–146.
3. Jiang CW, Green MA: **Silicon quantum dot superlattices: modeling of energy bands, densities of states, and mobilities for silicon tandem solar cell applications.** *J Appl Phys* 2006, **99:**114902.
4. Park N-M, Kim T-S, Park S-J: **Band gap engineering of amorphous silicon quantum dots for light-emitting diodes.** *Appl Phys Lett* 2001, **78:**2575–2577.
5. Cho E-C, Park S, Hao X, Song D, Conibeer G, Park SC, Green MA: **Silicon quantum dot/crystalline silicon solar cells.** *Nanotechnology* 2008, **19:**245201.
6. Cheng Q, Xu S, Long J, Ostrikov K: **Deterministic plasma-aided synthesis of high-quality nanoislanded nc-SiC films.** *Appl Phys Lett* 2007, **90:**173112.
7. Kurokawa Y, Tomita S, Miyajima S, Yamada A, Konagai M: **Photoluminescence from silicon quantum dots in Si quantum dots/ amorphous SiC superlattice.** *Jpn J Appl Phys* 2007, **46:**L833–L835.
8. Song D, Cho E-C, Conibeer G, Flynn C, Huang Y, Green MA: **Structural, electrical and photovoltaic characterization of Si nanocrystals embedded SiC matrix and Si nanocrystals/c-Si heterojunction devices.** *Sol Energy Mater Sol Cells* 2008, **92:**474–481.
9. Wang YQ, Wang YG, Cao L, Cao ZX: **High-efficiency visible photoluminescence from amorphous silicon nanoparticles embedded in silicon nitride.** *Appl Phys Lett* 2003, **83:**3474–3476.
10. Kim T-Y, Park N-M, Kim K-H, Sung GY, Ok Y-W, Seong T-Y, Choi C-J: **Quantum confinement effect of silicon nanocrystals *in situ* grown in silicon nitride films.** *Appl Phys Lett* 2004, **85:**5355–5357.
11. Kim T-Y, Park N-M, Choi C-J, Huh C, Ahn C-G, Sung GY, You I-K, Suemitsu M: **Effects of the hole tunneling barrier width on the electrical characteristic**

in silicon quantum dots light-emitting diodes. *Jpn J Appl Phys* 2011, **50:**04DG11.
12. Kim T-Y, Park N-M, Choi C-J, Kim A, You I-K, Suemitsu M: **Comparative study of silicon quantum dot formation *in-situ* grown with a gas mixture of SiH_4+N_2 and SiH_4+NH_3.** *J Korean Phys Soc* 2011, **59:**308–311.
13. Bandet J, Despax B, Caumont M: **Vibrational and electronic properties of stabilized wurtzite-like silicon.** *J Phys D: Appl Phys* 2002, **35:**234–239.
14. Zhang Y, Iqbal Z, Vijayalakshmi S, Grebel H: **Stable hexagonal-wurtzite silicon phase by laser ablation.** *Appl Phys Lett* 1999, **75:**2758–2760.
15. Kumar KUM, Krishna MG: **Chromium-induced nanocrystallization of a-Si thin films into the Wurtzite structure.** *J Nanomaterials* 2008. doi:10.1155/736534.
16. Yeh C-Y, Lu ZW, Froyen S, Zunger A: **Zinc-blende-wurtzite polytypism in semiconductors.** *Phys Rev B* 1992, **46:**10086–10097.
17. Kaneko T, Nemoto D, Horiguchi A, Miyakawa N: **FTIR analysis of a-SiC:H films grown by plasma enhanced CVD.** *J Crystal Growth* 2005, **275:**e1097–e1101.
18. Kim HY, Shao Q, Kim Y-H: **Characterization of low-dielectric-constant SiOC thin films deposited by PECVD for interlayer dielectrics of multilevel interconnection.** *Surf Coat Technol* 2003, **171:**39–45.
19. Lucovsky G, Niimi H: **Remote plasma-assisted oxidation of SiC: a low temperature process for SiC–SiO_2 interface formation that eliminates interfacial Si oxycarbide transition regions.** *J Phys Condens Matter* 2004, **16:**S1815–S1837.
20. Edelberg E, Bergh S, Naone R, Hall M, Aydil ES: **Luminescence from plasma deposited silicon films.** *J Appl Phys* 1997, **81:**2410–2417.
21. Sung GY, Park N-M, Shin J-H, Kim K-H, Kim T-Y, Cho KS, Huh C: **Physics and device structures of highly efficient silicon quantum dots based silicon nitride light-emitting diodes.** *IEEE J Sel Top Quant Electron* 2006, **12:**1545–1555.
22. Wolkin MV, Jorne J, Fauchet PM, Allan G, Delerue C: **Electronic states and luminescence in porous silicon quantum dots: the role of oxygen.** *Phys Revi Lett* 1999, **82:**197–200.
23. Nevin WA, Yamagishi H, Yamguchi M, Tawada Y: **Emission of blue light from hydrogenated amorphous silicon carbide.** *Nature* 1994, **368:**529–531.
24. Ma T, Xu J, Chen K, Du J, Li W, Huang X: **Red-green-blue light emission from hydrogenated amorphous silicon carbide films prepared by using organic compound xylene as carbon source.** *Appl Phys Lett* 1998, **72:**13–15.
25. Joannopoulos JD, Cohen ML: **Electronic properties of complex crystalline and amorphous phases of Ge and Si. I. Density of states and band structures.** *Phys Rev B* 1973, **7:**2644–2657.

doi:10.1186/1556-276X-7-634
Cite this article as: Kim *et al.*: ***In situ*-grown hexagonal silicon nanocrystals in silicon carbide-based films.** *Nanoscale Research Letters* 2012 **7**:634.

Submit your manuscript to a SpringerOpen journal and benefit from:

► Convenient online submission
► Rigorous peer review
► Immediate publication on acceptance
► Open access: articles freely available online
► High visibility within the field
► Retaining the copyright to your article

Submit your next manuscript at ► springeropen.com